nature REVIEWS DRUG DISCOVERY

SUPPLEMENTARY INFORMATION

In format as provided by the authors

Advances in therapeutic peptides targeting G protein-coupled receptors

Anthony P. Davenport, Conor C. G. Scully, Chris de Graaf, Alastair J. H. Brown and Janet J. Maguire

https://doi.org/10.1038/s41573-020-0062-z

Supplementary Text

Insights from structural studies

Currently experimental X-ray crystallography or cryo-electron microscopy (cryoEM) structures have been reported for the seven-transmembrane domain (7TM) domains of 62 GPCRs, covering 212 distinct GPCR-ligand complexes and 200 unique ligands. Structures of 27 peptide or protein binding GPCRs have been reported, covering 65 unique receptor-ligand complexes. Twenty two of the experimentally determined GPCR structures (10%) contain a peptide ligand, covering Class A GPCRs apelin, angiotensin AT_1 and AT_2, complement $C5a_1$, endothelin ET_B, neurotensin NTS_1,opioid receptors δ (DOR) and MOR, chemokine CCR5, CXCR4 and US28 receptors and Class B GPCRs calcitonin CT, CGRP, glucagon, GLP-1, and parathyroid PTH1 receptors (Supplementary Table 1, Figures 2 and 4). The Supplementary Table 1 and Supplementary Figure 1 show how the peptide bound structures of AT_1, AT_2, ET_B, CT, DOR, MOR, CXCR4, CT, CGRP, glucagon, GLP-1 and PTH1 receptors provide structural templates and detailed insights into the structural determinants of ligand binding and functional activity (Box 3). This is shown for four identical and 21 homologous therapeutically relevant peptides, covering four of the 10 clinically relevant endogenous peptide ligands (Table 1), 15 of the 40 synthetic peptide drugs (Table 2) and six of the 11 peptide ligands that are currently in development (Table 3). The structures of several of the previously mentioned receptors, as well as neuropeptide $NPYY_1$, KOR, NOP, CT and corticotropin releasing factor CRF_1 receptors provide templates to model the three-dimensional binding modes of an additional 32 clinically relevant peptides to these and/or closely related receptors (Supplementary Table 1). The accumulated portion of GPCR-peptide complexes that can be structurally modelled based on homologous peptides and/or receptors covers about half of all clinically relevant peptides reported in Tables 1, 2 and 3. The following section summarises the binding modes of these GPCR-peptide complexes (Supplementary Table 1, Supplementary Figure 1, Figures 2 and 4) providing insights into the structural determinants of binding and functional activity (Box 3) of several of these clinically relevant peptides and representing potential templates for the structure-based optimisation and design of novel GPCR peptide therapeutics.

Figures 2, 4 and Supplementary Figure 1 show how peptide ligands adopt diverse binding modes across GPCRs, reflecting the diverse chemical structures and properties of both ligands and receptor binding sites. Class A GPCR peptide ligands generally target ECL2 and a polar/ionic interaction site at the top of TM6/7/ECL3 and bind differentially located and shaped lipophilic regions deeper in the 7TM receptor pocket. Helical Class B GPCR ligands share an apolar interaction site with the region between TM1/2/7 that is less accessible in Class A GPCRs, but form differential polar interaction networks associated with

different relative orientations of the extracellular N-terminal domain (ECD) and the 7TM domain[1].

The octapeptide Ang II [Sar[1], Ile[8]] partial agonist bound AT_1 and AT_2 crystal structures[122,123] show an extensive polar interaction network between C_{ter}-K^{5x43}, Tyr[4]-F/M^{45x52}, His[6]/Pro[7]-R$^{4.63x64}$, Arg[2]-D^{6x58}/D^{7x31}, whereas Ile[1] and Pro[7] target lipophilic hotspots between W^{2x60}, V/L^{3x32} and I$^{7.39x38}$ (Supplementary Table 1, Figures 2-3). The conformation of Ang II [Sar[1], Ile[8]] is stabilised by aromatic stacking between Tyr[4] and His[6] and an intramolecular H-bond between Tyr[4] and the C-terminus. Comparative analysis of different conformational states of antagonist and agonist bound AT_1 and AT_2 structures (Supplementary Table 1), combined with biophysical and pharmacological studies provide insights into determinants of biased angiotensin receptor signalling (Box 3). The homologous clinically relevant natural peptide angiotensin-II, Aclerastide (discontinued Phase 3) and TRV027 (discontinued Phase 2) (Table 1, Table 3, Figure 2) likely adopt similar binding modes in AT_1.

The apelin receptor structure[121](Figure 4) shows how the 17-amino acid apelin mimetic peptide agonist AMG3054 adopts binding mode targeting the major pocket in the 7TM domain and the top of ECL 1 and ECL 2 (Supplementary Table 1, Figures 2 and 3, Supplementary Figure 1) and provides a structural template to identify determinants of biased apelin signalling (Box 3). The C-terminal carboxylic acid group of the apelin mimetic interacts with the cationic R168^{ECL2} and K268^{6x55} residues. The C-terminal chlorinated phenyl residue is stacked between Y35^{1x39}, W85^{2x60}, Y88^{2x63}, Y299$^{7.43x42}$ and forms a halogen bond with the backbone carbonyl of W85^{2x60}. Nle[15] binds another lipophilic region between Y271$^{6.58}$ and F290$^{7.34}$. The identified structural determinants are consistent with apelin mutation studies[121], showing the importance of for example of Y35^{1x39}, W85^{2x60}, and R168^{ECL2}, suggesting that features of the AMG3504 binding mode are transferrable to apelin analogues.

The endothelin ET_B receptor structure[125] shows how the C-terminus of the 21-residue endothelin-1 (ET-1) peptide targets lipophilic pockets in the major pocket of ET_B, whereas the extra-cellular vestibule of the receptor folds around the α-helix and N-terminus of the peptide ligand (Supplementary Table 1, Figures 2 and 4, Supplementary Figure 1). The C-terminal carboxylic acid group of ET-1 forms a tight ionic H-bond interaction network with the cationic K182^{3x33}, K273$^{5.39x38}$, and R343^{6x55} residues, whereas the N-terminal Cys[1] and Ser[2] residues form polar interactions with the backbone of L257^{45x52} in EL2. The C-terminal Trp[21] and Ile[20] residues of ET-1 bind a lipophilic pockets between TM5/6 (L277$^{5.42x43}$, W336^{6x48}, I339^{6x51}) and TM2/3/EL1 (W167^{23x50}, I181^{3x32} and Y148^{3x33}.), respectively. The conformation of ET is stabilised by disulfide bridges between the Cys[1] and Cys[15] and between Cys[3] and Cys[11]. The homologous shorter 14-mer SPI-1620 (discontinued Phase 2, Table 3, Figure 2)

is expected to adopt a similar binding mode in ET_A as the C-terminal region of ET-1 in the ET_B structure, consistent with mutation studies[125].

The pentapeptide agonist DAMGO adopts a binding mode in the MOR cryoEM structure[128] in which the N-terminal Tyr^1 forms ionic interactions with $D147^{3x32}$ and targets a small lipophilic region between $I296^{6x51}$, $H278^{6x52}$ and $V281^{6x55}$ (Supplementary Table 1, Figures 2-3). The $MePhe^4$ residue of DAMGO targets a second lipophilic hotspot between $W133^{23x50}$, $P143^{3.28}$ and $I144^{3x29}$. The Tyr^1 and Phe^4 residues of the dual DOR/MOR pentapeptide agonist Met-enkephalin (Tyr^1-Gly^2-Gly^3-Phe^4-Met^5, Ph2) Table 3, Figure 2) are expected to adopt a similar DOR/MOR binding mode as the Tyr^1 and $MePhe^4$ residues of DAMGO.

The CXCR4 chemokine receptor structure (Supplementary Table 1, Figure 4)[130] shows how positively charged arginine residues of the cyclic 16-mer peptide antagonist CVX15 form ionic/H-bond interaction networks with CXCR4 (Arg^1-$D187^{45.51}$, Arg^2-$T117^{3.33}$/$D171^{4.61x60}$, Arg^{11}-$D272^{6x58}$/$D277^{7.31x30}$), while the naphthalene moiety of Aln^3 binds a lipophilic pocket formed by $Y190^{45x54}$/$F199^{5.39x38}$/$H203^{5.42x43}$/$I259^{6x55}$. The beta-strand conformation of CVX15 is further stabilised by a disulfide bridges between the Cys^4 and Cys^{13}. The homologous 15-mer BL-8040 (Phase 3, Table 3, Figure 2) is expected to adopt a similar binding mode in CXCR4, targeting an additional lipophilic pocket between $W94^{2x60}$, $V112^{3x28}$, $H113^{3x29}$ with its additional N-terminal 4-fluorinated benzyl residue, potentially forming additional intra/intermolecular ionic interactions with its C-terminal diaminopropoanoic acid residue. The binding mode of CVX15/BL-8084 to CXCR4 is distinct from the binding mode of chemokine ligands which bind the receptor N-terminus with their conserved disulfide stabilised C-terminal region and target different lipophilic regions in the TM pocket[2] as observed in CCL5 bound CCR5[129] (Figure 3), vMIP-II bound CXCR4, and CX3CL1 bound US28[132, 3] 8 new crystal structures.

The PMX53 bound $C5a_1$ crystal structure[124] shows how the C-terminal Arg^6 residue of the discontinued (Phase 1A/2B) hexamer peptide antagonist PMX53 forms polar interactions with Y^{6x51} and $D^{7.35x34}$, while the apolar Phe^1 and $dCha^4$/Trp_5 residues target lipophilic regions between $R264^{EL2}$/$C274^{45x50}$/$V276^{45x52}$ and between $L278^{2x60}$/$I182^{2x64}$/$P199^{3x29}$/$C274^{45x50}$/$C369^{7.36x35}$, respectively (Figure 2, Figure 3).

The peptidomimetic antagonist UR-MK299 forms H-bond interactions with $Q219^{5x461}$, $N283^{6x55}$ and $D286^{6.58}$ and targets lipophilic regions between in the neuropeptide $NPYY_1$ crystal structure[141](Figure 3), providing a structural template (Supplementary Table 1) for modelling the binding mode of the N-terminal Arg-Try residues of Obinepitide and TM30339 (Table 3, discontinued Phase 2) in homologous $NPYY_2$/$NPYY_4$.

Class B GPCRs comprise an ECD of 120–160 residues and a 7TM of 310–420 residues. In addition to the 7TM and full length (7TM and ECD) structures of class B GPCRs

described below several structures of isolated class B GPCR ECDs have been solved[149](Supplementary Table 1), including calcitonin analogue bound CT receptor[144], GIP bound GIP receptor[4] and GLP-1, Ex[9-39] and semaglutide bound GLP-1 receptor[25,5,6]. These ECD-peptide complexes show conserved hydrophobic interactions between conserved apolar residues in the C-terminal part of the ligand (such as GLP-1: Phe^{28}, Ile^{29}, Leu^{32}) and similar hydrophobic interaction sites with the ECD of the corresponding receptor (for example, GLP-1 receptor: L32, T35, V36, and W39^{ECD} in α_1; Y69^{ECD} in β turn 1 connecting β1–β2; Y88, L89, and P90 in β turn 2 connecting β3–β4)[149].

The full-length calcitonin-like receptor (CLR) cryoEM structure shows how the C-terminal region of the agonist CGRP binds the ECD, while the N-terminal helical region binds the 7TM domain of CLR[133]. The N-terminal Phe^{36} targets a hydrophobic pocket between G71^{ECD}/W72^{ECD} in CLR and W84/P85 of RAMP1. The CLR/CGRP/RAMP1 complex is further stabilised by amongst others polar interaction networks between N-terminal amide group of CGRP and T122^{ECD} and between Lys^{35} (CGRP), R119^{ECD} (CLR), and W84 (RAMP2), consistent with the function of RAMP1 as allosteric modulator of CLR. Val^{8} (F349^{6x53}/M369^{7x41}/H370^{7x42}/M373^{7x45}) and Leu^{12}/Leu^{16} (V135^{1X35}/A138^{1x36}/ L139^{1x37}/L141^{1x39}/F142^{1x40}/L195^{2x68}/a199^{2x72}/H370^{7x42}) in the C-terminal helix of CGRP target lipophilic regions in CLR, consistent with SAR and mutation studies showing the role of several of these residue in CGRP-peptide binding[133] (Figure 3). The CGRP bound CLR structure provides a structural basis for modelling the binding mode of several homologous clinically relevant peptides to CLR and/or CR receptors and RAMP bound AMY$_{1/2/3}$ complexes, including adrenomedullin, calcitonin, Davalintide, Elcatonin, and Pramlintide (Tables 1, 2, Supplementary Table 1 and Figure 2).

The agonist 31-mer GLP-1, biased agonist 36-mer Ex-P5, and truncated agonist 15-mer peptide 5 adopt a similar overall binding conformation and orientation within the 7TM domain of full-length GLP-1 receptor X-ray crystallography and cryoEM structures, but show different structural interaction patterns[133,136,137,149](Figure 2 and 4, Supplementary Figure 1). Val3 and Val7 of Ex-P5 and the fluorinated Phe12 homolog X_1 and the gem-dimethyl of peptide 5 target the same lipophilic pocket defined (L141^{1x36}, L144^{1x39}, Y145^{1x40}, Y148^{1x43}, L384^{7x38}, E387^{7x41}, L388^{7x42}). In the lower resolution GLP-1 bound cryoEM structure the homologous Phe12 and Val16 are located at a similar position, but TM1 seems to be rotated, with for example, L144^{1x39} and Y148^{1x43} towards the membrane. The substituted biphenyl residue X_2 of peptide 5 extends between TM1 (L142^{1x37}/Y145^{1x40}) and TM2 (L201^{2x72}/K202^{2x73}), whereas the L-Norvalin derivative X_3 of peptide 5 further extends between the ECD (L32), TM2 (M204^{2x75}), ECL2 (C296^{45x50}), targeting additional lipophilic regions to compensate for the limited interaction with the ECD and explaining the similar

potency of peptide 5 compared to GLP-1. Ex-P5 and peptide 5 share polar interactions with R299^{45x53} and R380$^{7.35b}$, and form ligand specific polar interactions with Y152^{1x47}/R190^{2x60} (peptide 5/c-tetrazole-Ala), R310$^{5.44}$ (Ex-P5/Glu^{1}), and E387$^{7.42b}$ (peptide 5/Cap1) that are not observed in the GLP-1-bound GLP-1 receptor structure. The binding modes of Ex-P5 and peptide 5 are consistent with GLP-1 receptor peptide ligand SAR and mutation studies and provide a template for the elucidation of determinants of biased signalling (Box 3) and for modelling structural interactions of the clinically relevant peptides glucagon, GLP-1, Albiglutide, Dulaglutide, Exendin-4, Liraglutide. Lixisenatid, Semaglutide, GTP-010, Taspoglutide, TT-223 with the GLP-1 receptor (Tables 1, 2, 4 Supplementary Table 1, Figure 2). The GLP-1 receptor-peptide ligand complexes furthermore can serve as basis for the construction of GLP-2 (Apraglutide, Elsiglutide, Glepaglutide,Teduglutide) and GIP (MAR701, MAR709) in complex with homologous peptide ligands, guided by SAR and mutagenesis studies[149] (Tables 1, 2, 4; Supplementary Table 1; Figure 2).

The Ser2/Phe6 and Val10 residues of the partial agonist NNC1702 target the same lipophilic pockets defined by TM1 and TM7 (Y138^{1x36}, F141^{1x39}, Y148^{1x43}, L382^{7x38}, D385^{7x41}, L386^{7x42}) and TM1/TM2 (Y138^{1x36}, L198^{2x72}) in full-length glucagon receptor[135] as the Ala8/Phe12 and Val16 homologs of GLP-1/Ex-P5/peptide 5 in the GLP-1 receptor structures described above. This glucagon receptor-peptide ligand binding mode is consistent with glucagon receptor ligand SAR and receptor mutation studies[149].

Also in the full-length PTH1 crystal structure[139] and cryoEM structures[140], ePTH (Aib3, Leu7) and PTH analogue (Ala3, Leu7), target the lipophilic pockets between TM1/2 (F184^{1x36}, L187^{1x39}, C191^{1x43}, M441^{7x38}, E444^{7x41}, M445^{7x42}), in line with PTH1 SAR and mutation studies[149]. The peptide bound PTH1 structures provide a template to model the interactions of PTH1/PTH2 receptors with PTH, PTHrP, Abaloparatide, Teriparatide, Ostabolin-C as well as the construction of homology models of GHRH with AKL-0707, DAC:GRs, Sermorelin, Tesamorelin (Tables 1, 2 and 4; Supplementary Table 1; Figure 2 and 4; Supplementary Figure 1)

Supplementary Figure 1

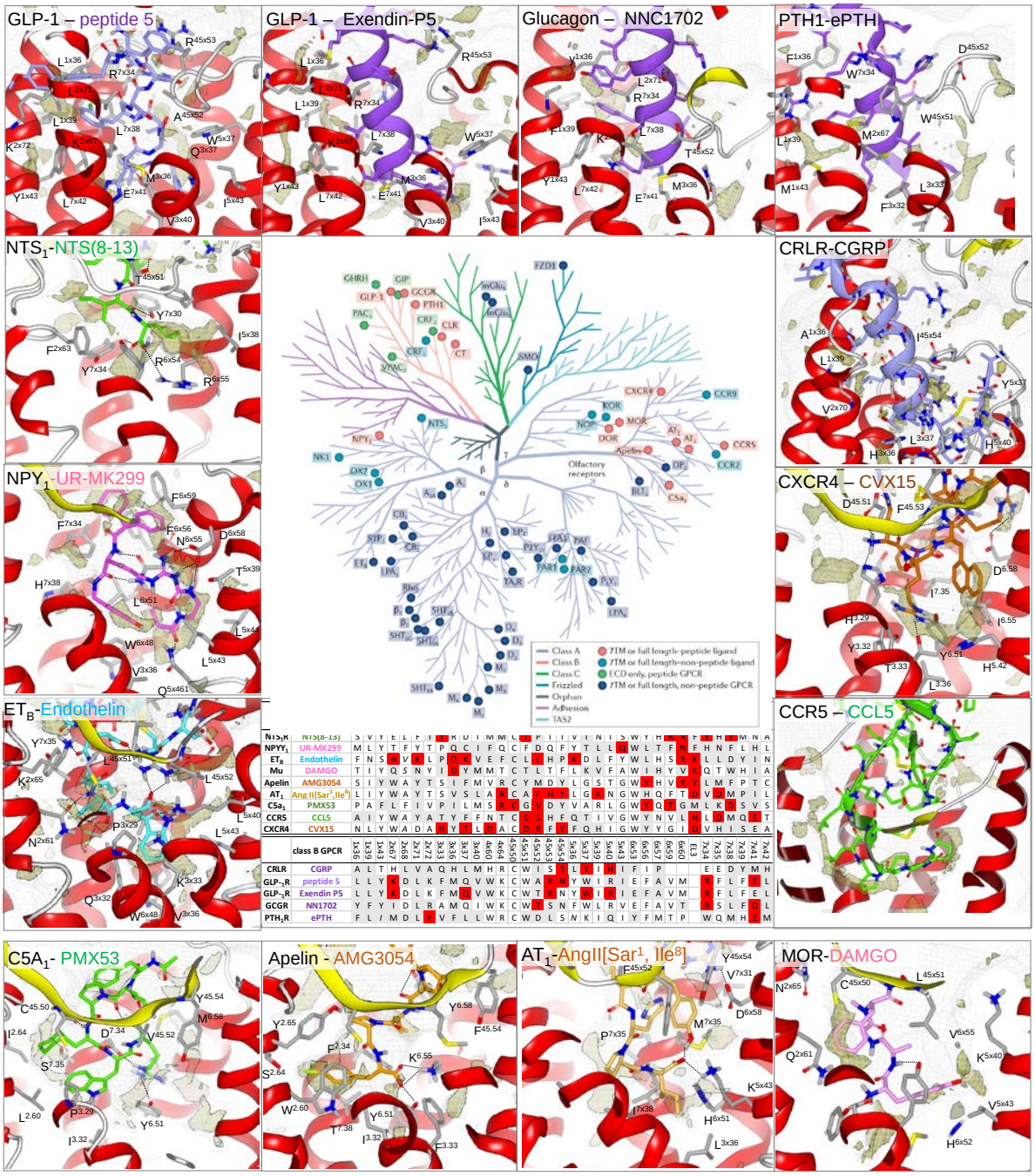

Supplementary Figure 1 | **X-ray crystallography and cryo-electron microscopy structures of GPCRs.** In the central GPCR phylogenetic tree peptide GPCRs for which 7TM/full-length structures are available in complex with peptide ligands (red) or only in complex with non-peptide ligands (yellow) are distinguished from peptide GPCRs for which only ECD structures are available (green) and non-peptide GPCRs for which 7TM/full-length structures are available (blue), consistent with Supplementary Table 1. Related GPCR families, Adhesion (purple), Glutamate (orange), Frizzled (light green) and Taste (dark green) are shown for reference. Receptors are classified as orphans when the endogenous

ligand(s) is not yet established. The bottom panel summarises structural interactions for aligned binding site residues of class A and class B peptide GPCRs forming polar H-bond or ionic interactions (red), or only lipophilic interactions (grey) with peptide ligands shown in the individual binding mode figure panels.

Binding sites of AMG3054 bound Apelin (PDB ID: 5VBL)[121], octapeptide Ang II [Sar^1, Ile^8] partial agonist bound angiotensin AT_1 (PDB: 6DO1)[122] Complement $C5a_1$ (PDB: 6C1Q)[124], Endothelin ET_B (PDB: 5GLH)[125], neurotensin NTS_1R (PDB: 3ZEV) [126], UR-MK299 bound neuropeptide $NPYY_1$ (PDB: 5ZBQ)[141], MOR (PDB: 6DDE)[128], chemokine CCR5 (PDB: 5UIW)[129] receptors, and class B GPCRs calcitonin Calcitonin gene-related peptide bound CGRP (PDB: 6E3Y)[134], NNC-1702 bound glucagon receptor (PDB: 5YQZ)[135], peptide 5 (PDB: 5NX2)[136] and Exendin-P5 (PDB: 6B3J)[135] bound GLP-1 receptor, and ePTH bound parathyroid PTH1 [139] receptors. Views are focused on the 7TM domain and consistent with the orientations of peptide diagrams shown in Figure 2. The binding pocket surfaces (grey mesh) are contoured at 1 kcal/mol using the C3 (carbon sp3) GRID probe[203], whereas lipophilic areas are defined using the C1= (lipophilic) probe contoured at -2.8 to -3.0 kcal/mol, customized to GPCR binding sites[204]. Generic GPCR residue numbers[205] are provided based on Ballesteros-Weinstein Class A GPCR (Apelin, AT_1, $C5a_1$, CCR5, ET_B, MOR, $NPYY_1$)[206] and Wootten[207] Class B GPCR (CGRP, Glucagon, GLP-1, $PTHR_1$) numbering schemes. According to these schemes, the first (1-7) denotes the transmembrane helix (TM), and the following number indicates the residue position relative to the most conserved amino-acid in the helix (which is assigned the number 50), considering numbering offset due to helical bulges or constrictions[205].

Supplementary Figure 2

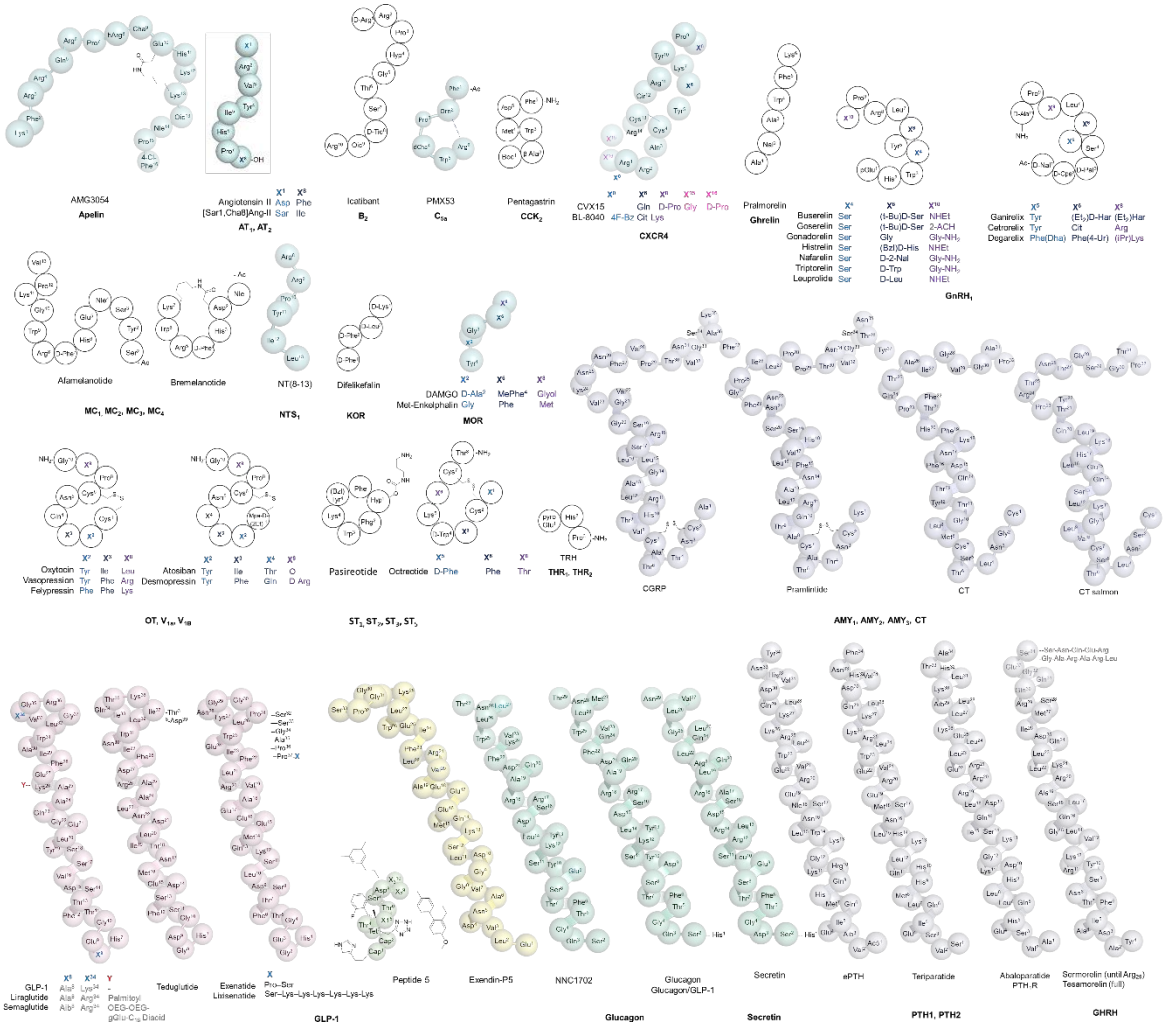

Supplementary Figure 2 | **2D and 3D diagrams of clinically relevant GPCR peptides (Table 1) and synthetic GPCR peptide drugs (Table 2).** Peptides are shown as beads based on the three-dimensional position of Cα atoms of structural templates of peptides bound to experimentally determined 7TM structures of associated GPCRs (Supplementary Table 1). The orientations of the 3D peptide bead strings are consistent with their binding mode in the GPCR binding site (Figure 3), assuming a view in which TM1 is on the left, TM5 is on the right, and the extra-cellular side is up. Peptides for which no 7TM GPCR structure bound 3D template is available, or depicted as 2D diagrams reflecting the putative structure based on (secondary) structure information of the free peptide, disulphide bridge constraints and binding mode information (showing an orientation consistent with the 3D diagrams).

Supplementary Table 1| **Experimentally determined structures of peptide binding GPCRs**

Family	Target Receptor	Ligand	Ligand mode of action	Similar peptide drug in Development	PDB
Class A					
Serotonin	$5HT_{2A}$	Risperidone	ANT	None	6A93
		Zotepine	ANT		6A94
Angiotensin	AT_1	Olmersartan	iAGO	None	4ZUD[195]
		ZD7155	ANT		4YAY[196]
		Ang II [Sar^1,^{8}Ile]	AGO		6DO1[122]
Angiotensin	AT_2	8EM	ANT	None	5UNH[121]
		8ES	ANT		5UNF[137]; 5UNG
		Ang II [Sar^1,^{8}Ile]*	AGO	Angiotensin II Aclerastide (AT_1), TRV120027 (AT_1)	5XJM[199]
Apelin	Apelin	AMG305	AGO	Apelin	5VBL[121]
Complement Peptide	$C5a_1$	NDT 9513727; PMX53	ANT alloANT		6C1Q[124]
		Avacopan; PMX53	ANT alloANT		6C1R[124]
		NDT 9513727	alloANT		5O9H
Endothelin	ET_B	Endothelin-1*	AGO	Endothelin 1, SPI-1620	5GLH; 5GLI[125]
		Bosentan	ANT	None	5XPR
		K-8794	ANT		5X93
Neuropeptide Y	Y_1	BMS-193885	ANT	None	5ZBH
		UR-MK299	ANT		5ZBQ
Neurotensin	NTS_1	$NT_{(8-13)}$*	AGO	Neurotensin	4XEE; 4XES; 3ZEV[126]; 4BUO; 4BV0; 4BWB; 4GRV; 5T04
opioid	δ	DIPP-NH_2*	ANT	None	4RWA; 4RWD[127]
		Naltrindole	ANT		4N6H; 4EJ4
	κ	MP1104	AGO	None	6B73[142]
		JDTic	ANT		4DJH
	μ	BU72	AGO	None	5C1M
		DAMGO*	AGO		6DDE; 6DDF [128]
		Morphinan	ANT		4DKL
	NOP	C-24	ANT	None	4EA3[143]
		C-35	ANT		5DHG
		SB-612111	ANT		5DHH

Orexin	OX_1	Suvorexant	ANT	None	4ZJ8
		SB-674042	iAGO		4ZJC
	OX_2	EMPA	ANT		5WQC; 5WS3
		Suvorexant	ANT		4S0V
Proteinase-Activated	PAR1	Vorapaxar	ANT	None	3VW7
	PAR2	AZ3451	ANT	None	5NDZ
		AZ8838	ANT		5NDD
		Fab*	ANT		5NJ6
Tachykinin	NK_1	Aprepitant	ANT	None	6HLO
		CP-99,994	ANT		6HLL
		L760735	ANT		6E59
		Netupitant	ANT		6HLP
Chemokine	CCR2	BMS-681; CCR2-RA-[R]	ANT; NAM	None	5T1A
		MK-0812	ANT		6GPS, 6GPX
	CCR5	Maraviroc	ANT	None	4MBS
		5P7-CCL5*	AGO	CCL3, CCL5	5UIW[129]
	CCR9	Vercirnon	ANT	None	5LWE
	CXCR4	IT1t	ANT	None	3ODU; 3OE6; 3OE8; 3OE9[130]
		CVX15*	ANT	BL-8040	3OE0[130]
		vMIP-II*	ANT	CXCL12	4RWS [131]
	US28	CX3CL1*	AGO	None	4XT1[*]; 4XT3[132]
		CX3CL1.35*	AGO		5WB2[151]
		Nb7[$]	AGO		5WB1[151]
	Class B				
Calcitonin	AM_1	Adrenomedullin*	AGO	Adrenomedullin	3AQF (ECD), 4RWF (ECD)
		CGRP analog*	AGO	CGRP	4RWG (ECD)
	CT	Calcitonin*	AGO	Calcitonin, Elcatonin	5UZ7
					5II0 (ECD)[144] 5UZ7[a]; 6NIY
	CGRP	CGRP*	AGO	CGRP	6E3Y[133]
		Apo		None	3N7P (ECD)
		Telcagepant; Olcegepant	ANT	None	3N7R (ECD)
		9968071l; Olcegepan	ANT		3N7S (ECD)
Corticotropin-releasing factor	CRF_1	CRF*	AGO	CRF, Corticorelin	3EHU[148], 2L27
		CP-376395	NAM	None	4K5Y[*145]; 4Z9G
	CRF_2	Astressin*	AGO	Astressin, Urocortin-1, Urocortin-2, RT-400, Stresscopin	3N93[146]
		Urocortin-1*	AGO		1U34[147]
		Urocortin-2*	AGO		3N96[146]

Glucagon	Glucagon	NNC1702*	AGO	Glucagon, GLP-1	5YQZ[135]
		ZP3780*	AGO		
		NNC0640 mAb1[$]	ANT		5XEZ; 5XF1[202]
		mAb1[$]	ANT		4ERS (ECD)
		NNC0640[a]	NAM		4L6R
		MK-0893	NAM		5EE7
	GLP-1	Exendin-P5*	AGO	Glucagon, GLP-1 Albiglutide, Dulaglutide, Exendin-4, Liraglutide. Lixisenatid, Semaglutide GTP-010, Taspoglutide, TT-223	6B3J[137]
		GLP-1[a*]	AGO		5VAI[133]
		Peptide 5*	ANT		5NX2[136]
		GLP-1*	AGO		3IOL (ECD)[154]
		Semaglutide*	AGO		4ZGM (ECD)[25]
		$Ex_{[9-39]}$*	ANT		3C59 (ECD)[153]
		Exendin-4 analog*	AGO		5OTT (ECD)
		Exendin-4 analog*	AGO		5OTU (ECD)
		Exendin-4 analog*	AGO		5OTV (ECD)
		Exendin-4 analog*	AGO		5OTW (ECD)
		Fab 3F52[$]	ANT	None	5E94 (ECD)
		NNC0640	NAM	None	5VEX
		PF-06372222	NAM		5VEW
	GIP	GIP*	AGO	GIP, MAR701, MAR709	2QKH (ECD)[152]
	GIP	Gipg013 Fab[$]	ANT	None	4HJ0 (ECD)
	GHRH	Apo		None	2XDG (ECD)
Parathyroid Hormone	PTH1	ePTH*	AGO	PTH, PTHrP Abaloparatide, Teriparatide, Ostabolin-C	6FJ3[139]
		PTH analog*	AGO		6NBF; 6NBH; 6NBI[140]
		PTH*	AGO		3C4M (ECD)
		PTHrP*	AGO		3H3G (ECD)
VIP and PACAP	PAC_1	$PACAP_{6–38}$*	ANT	None	2JOD, 1GEA (ECD)
		Apo			3N94 (ECD)
	$VPAC_2$	Apo			2X57 (ECD)

[a)] Ligand included in crystallisation studies, but ligand coordinates not determined or low resolution (<4Å). [b)] The following ligand types are defined: Full agonist (AGO), partial agonist (pAGO) inverse agonist (iAGO), antagonist (ANT) and negative allosteric modulators (NAM). [c)] Peptide ligands are indicated with "P", antibodies with ('Ab'), other ligands are small molecules. [d)] Endogeneous peptides and endogeneous/synthetic peptide drugs/in development indicated in Tables 1-3 that share sequence/structural similarity to the peptide ligand in the experimentally determined (X-ray crystallography, cryoEM, NMR) structure. [e)] Assessment of structural receptor-peptide ligand models including endogeneous and/or clinically relevant peptide ligands (Table 1-3) that can be constructed by combining the specified structural templates (with indicated additional templates indicated between brackets). [f)] Structures of truncated Extracellular Domain are indicated with 'ECD' between brackets, other structures contain transmembrane domain. Protein Data Bank[200, 201] (PDB) ID codes of experimentally determined structures (crystallography, cryo-EM) of complexes of peptide ligands bound to the full-length transmembrane domain (TM-peptide) or extracellular domain (ECD-peptide) of the receptor, as well as non-peptide ligands bound to the receptor transmembrane domain (TM). Structures of free peptide ligands (NMR, crystallography) are only reported for receptors for which no peptide ligand structures are available.

References

115. Dal Maso E, Just R, Hick C, Christopoulos A, Sexton PM, Wootten D, Furness SGB. Characterization of signalling and regulation of common calcitonin receptor splice variants and polymorphisms. *Biochem Pharmacol* **148**,111-129 (2018).
116. Dal Maso E, Zhu Y, Pham V, Reynolds CA, Deganutti G, Hick CA, Yang D, Christopoulos A, Hay DL, Wang MW, Sexton PM, Furness SGB, Wootten D. Extracellular loops 2 and 3 of the calcitonin receptor selectively modify agonist binding and efficacy. *Biochem Pharmacol* **150**, 214-244 (2018).
119. Vass, M. *et al.* Chemical Diversity in the G Protein-Coupled Receptor Superfamily. *Trends Pharmacol Sci* **39,** 494-512 (2018).
120. Pandy-Szekeres, G. *et al.* GPCRdb in 2018: adding GPCR structure models and ligands. *Nucleic Acids Res* **46,** D440-D446 (2018)
121. Ma, Y. *et al.* Structural Basis for Apelin Control of the Human Apelin Receptor. *Structure* **25,** 858-866 e854 (2017).
122. Wingler, L. M., McMahon, C., Staus, D. P., Lefkowitz, R. J. & Kruse, A. C. Distinctive Activation Mechanism for Angiotensin Receptor Revealed by a Synthetic nanobody. *Cell* **176,** 479-490 e412 (2019).

123. Zhang, H. *et al.* Structural basis for selectivity and diversity in angiotensin II receptors. *Nature* **544,** 327-332 (2017).
124. Liu, H. *et al.* Orthosteric and allosteric action of the C5a receptor antagonists. *Nat Struct Mol Biol* **25,** 472-481 (2018).
125. Shihoya, W. *et al.* Activation mechanism of endothelin ETB receptor by endothelin-1. *Nature* **537,** 363-368 (2016).
126. White, J. F. *et al.* Structure of the agonist-bound neurotensin receptor. *Nature* **490,** 508-513 (2012).
127. Fenalti, G. *et al.* Structural basis for bifunctional peptide recognition at human delta-opioid receptor. *Nat Struct Mol Biol* **22,** 265-268 (2015).
128. Koehl, A. *et al.* Structure of the mu-opioid receptor-Gi protein complex. *Nature* **558,** 547-552 (2018).
129. Zheng, Y. *et al.* Structure of CC Chemokine Receptor 5 with a Potent Chemokine Antagonist Reveals Mechanisms of Chemokine Recognition and Molecular Mimicry by HIV. *Immunity* **46,** 1005-1017 e1005 (2017).
130. Wu, B. *et al.* Structures of the CXCR4 chemokine GPCR with small-molecule and cyclic peptide antagonists. *Science* **330,** 1066-1071 (2010).
131. Qin, L. *et al.* Structural biology. Crystal structure of the chemokine receptor CXCR4 in complex with a viral chemokine. *Science* **347,** 1117-1122 (2015).
132. Burg, J. S. *et al.* Structural biology. Structural basis for chemokine recognition and activation of a viral G protein-coupled receptor. *Science* **347,** 1113-1117 (2015).
133. Liang, Y. L. et al. Phase-plate cryo-EM structure of a class B GPCR-G-protein complex. *Nature* **546**, 118-123 (2017).
134. Liang, Y. L. *et al.* Cryo-EM structure of the active, Gs-protein complexed, human CGRP receptor. *Nature* **561,** 492-497 (2018).
135. Zhang, H. *et al.* Structure of the glucagon receptor in complex with a glucagon analogue. *Nature* **553,** 106-110 (2018).
136. Jazayeri, A. *et al.* Crystal structure of the GLP-1 receptor bound to a peptide agonist. *Nature* **546,** 254-258 (2017).
137. Zhang, Y. *et al.* Cryo-EM structure of the activated GLP-1 receptor in complex with a G protein. *Nature* **546,** 248-253 (2017).
138. Liang, Y. L. *et al.* Phase-plate cryo-EM structure of a biased agonist-bound human GLP-1 receptor-Gs complex. *Nature* **555,** 121-125 (2018).
139. Ehrenmann, J. *et al.* High-resolution crystal structure of parathyroid hormone 1 receptor in complex with a peptide agonist. *Nat Struct Mol Biol* **25,** 1086-1092 (2018).

140. Zhao, L. H. *et al.* Structure and dynamics of the active human parathyroid hormone receptor-1. *Science* **364,** 148-153 (2019).
141. Yang, Z. *et al.* Structural basis of ligand binding modes at the neuropeptide Y Y1 receptor. *Nature* **556,** 520-524 (2018).
142. Che, T. *et al.* Structure of the Nanobody-Stabilized Active State of the Kappa Opioid Receptor. *Cell* **172,** 55-67 e15 (2018).
143. Thompson, A. A. *et al.* Structure of the nociceptin/orphanin FQ receptor in complex with a peptide mimetic. *Nature* **485,** 395-399 (2012).
144. Johansson, E. *et al.* Type II Turn of Receptor-bound Salmon Calcitonin Revealed by X-ray Crystallography. *J Biol Chem* **291,** 13689-13698 (2016).
145. Hollenstein, K. et al. Structure of class B GPCR corticotropin-releasing factor receptor 1. *Nature* **499**, 438-443 (2013).
146. Pal, K., Swaminathan, K., Xu, H. E. & Pioszak, A. A. Structural basis for hormone recognition by the Human CRFR2 G protein-coupled receptor. *J Biol Chem* **285,** 40351-40361 (2010).
147. Grace, C. R. *et al.* NMR structure and peptide hormone binding site of the first extracellular domain of a type B1 G protein-coupled receptor. *Proc Natl Acad Sci U S A* **101,** 12836-12841 (2004).
148. Kusano, S. *et al.* Structural basis for extracellular interactions between calcitonin receptor-like receptor and receptor activity-modifying protein 2 for adrenomedullin-specific binding. *Protein Sci* **21,** 199-210 (2012).
149. de Graaf, C. *et al.* Extending the Structural View of Class B GPCRs. *Trends Biochem Sci* **42,** 946-960 (2017).
150. Arimont, M. *et al.* Structural Analysis of Chemokine Receptor-Ligand Interactions. *J Med Chem* **60,** 4735-4779 (2017).
151. Miles, T. F. *et al.* Viral GPCR US28 can signal in response to chemokine agonists of nearly unlimited structural degeneracy. *Elife* **7,** (2018).
152. Parthier, C. *et al.* Crystal structure of the incretin-bound extracellular domain of a G protein-coupled receptor. *Proc Natl Acad Sci U S A* **104,** 13942-13947 (2007).
153. Runge, S., Thogersen, H., Madsen, K., Lau, J. & Rudolph, R. Crystal structure of the ligand-bound glucagon-like peptide-1 receptor extracellular domain. *J Biol Chem* **283,** 11340-11347 (2008).
154. Underwood, C. R. *et al.* Crystal structure of glucagon-like peptide-1 in complex with the extracellular domain of the glucagon-like peptide-1 receptor. *J Biol Chem* **285,** 723-730 (2010).

155. de Graaf, C. *et al.* Glucagon-Like Peptide-1 and Its Class B G Protein-Coupled Receptors: A Long March to Therapeutic Successes. *Pharmacol Rev* **68,** 954-1013 (2016).
156. Siu, F. Y. *et al.* Structure of the human glucagon class B G-protein-coupled receptor. *Nature* **499,** 444-449 (2013).
157. Gardella, T. J. & Vilardaga, J. P. International Union of Basic and Clinical Pharmacology. XCIII. The parathyroid hormone receptors--family B G protein-coupled receptors. *Pharmacol Rev* **67,** 310-337 (2015).
195. Zhang, H. *et al.* Structure of the Angiotensin receptor revealed by serial femtosecond crystallography. *Cell* **161,** 833-844 (2015).
196. Ban, T. *et al.* GPCR structure and function relationship: identification of a biased apelin receptor mutant. *Biochem J* **475,** 3813-3826 (2018).
197. Koole, C. *et al.* Second extracellular loop of human glucagon-like peptide-1 receptor (GLP-1R) has a critical role in GLP-1 peptide binding and receptor activation. *J Biol Chem* **287,** 3642-3658 (2012).
199. Asada, H. et al. Crystal structure of the human angiotensin II type 2 receptor bound to an angiotensin II analog. Nat Struct Mol Biol 25, 570-576 (2018).
200. RCSB Protein Data Bank. https://www.rcsb.org (2019)
201. H.M. Berman, J. Westbrook, Z. Feng, G. Gilliland, T.N. Bhat, H. Weissig, I.N. Shindyalov, P.E. Bourne. The Protein Data Bank Nucleic Acids Research **28,** 235-242 (2000).
202. Hilger, D. *et al.* Structural insights into ligand efficacy and activation of the glucagon receptor. *BioRXiv.* https://www.biorxiv.org/content/10.1101/660837v1.article-info
203. Goodford, P. J. A computational procedure for determining energetically favorable binding sites on biologically important macromolecules. *J Med Chem* **28,** 849-857 (1985).
204. Mason, J. S., High end GPCR design: crafted ligand design and druggability analysis using protein structure, lipophilic hotspots and explicit water networks." *In Silico Pharmacol* **1 23,** (2013).
205. Isberg, V. *et al.* Generic GPCR residue numbers - aligning topology maps while minding the gaps. *Trends Pharmacol Sci* **36,** 22-31 (2015).

206. Konvicka, K., Guarnieri, F., Ballesteros, J. A. & Weinstein, H. A proposed structure for transmembrane segment 7 of G protein-coupled receptors incorporating an asn-Pro/Asp-Pro motif. *Biophys J* **75,** 601-611 (1998).
207. Wootten, D., Christopoulos, A. & Sexton, P. M. Emerging paradigms in GPCR allostery: implications for drug discovery. *Nat Rev Drug Discov* **12,** 630-644 (2013).

Supplementary Table 2| **Endogenous peptides targeting Class A and B GPCRs that are approved for clinical use**

Family	Target Receptor	Ligand/ Approval Date	Clinical Indication	Affinity pK_i *pK_d **pIC_{50}	Potency pEC_{50}	Plasma half-life iv (min)	Volume of distribution (L)	Plasma binding (%)	Synonym Ligand peptide
Class A									
Angiotensin	AT_1 AT_2	Angiotensin II 2017	Septic shock	8.8 *10.2	9.0–9.3 -	< 1	-	-	Giapreza LJPC501
Melanocortin	MC_2	Cosyntropin 1967	Diagnosis, adrenal insufficiency	-	-	15	-	-	Tetracosactide
Thyrotropin-Releasing Hormone	TRH_1 TRH_2	TRH 1976	Testing Response of Anterior Pituitary, GI and in Secondary Hypothyroidism, Acromegaly.	†7.4 †7.4	8.5 -	5.3	15.7	-	Thyroliberin Protirelin
Vasopressin and Oxytocin	OT V_{1A} V_{1B} V_2	Oxytocin 1980	Induction of Labour	8.2–9.6 6.9–8.3 5.7–7.0 5.4–6.8	7.8-10.4 8 6.6-7.6 8.1	1-6	12.2	Negligible	Otx Pitocin Syntocinon
	OT V_{1A} V_{1B} V_2	Vasopressin 2014		7.3–9.3 8.5-9.3 9.9 7.9-9.1	- 9-9.6 8.3-8.7 10.3	10-20	9.8	Negligible	ADH Antidiuretic Hormone Arginine Vasopressin Argipressin
Class B									
Calcitonin	AMY_1 AMY_2 AMY_3 CT	Calcitonin 1981	Paget's Disease	- - - 9	8.9–11.3 11.4 8.0–10.6 9.0–11.2	10-38	4.9	-	Thyrocalcitonin LS-173874
Glucagon	GLP-1 Glucagon	Glucagon 1998	Severe Hypoglycaemia	6.9-7.0 -	- 9.0	8-18	17.5	-	
	Secretin	Secretin 2004	Diagnostic	-	9.7	45	2.7	-	
Parathyroid Hormone	PTH1 PTH2	PTH 2006	Hypocalcaemia, Parathyroid Deficiency	-	-	90	5.4	Negligible	Natpara, ALX1-11, rhPTH(1-84), **Note 1**
	PTH1 PTH2	Teriparatide 2002	Post-Menopausal Osteoporosis	**7.4 **7.7-7.8	- -	5	8.4	-	**Note 1**

Identification of endogenous peptides approved for clinical use was identified from the GuidetoPharmacology database. This has the most extensive classification with other groups being antibodies, natural products, metabolites or synthetic organics. The list was compared with DrugBank with further information from RxList Global Data or relevant company websites.

Pharmacokinetic and pharmacodynamics parameters were curated from GuidetoPharmacology, DrugBank as well as original citations. The peptides identified in use in any geographical region, will largely reflect those used widely in major pharmaceutical markets such as North America, Asia and Europe but may not capture peptides licensed in just one country.

Class, Target receptor and Ligand. Unlike small molecules that may target multiple receptors**,** the table reflects the consensus that peptides act primarily on a single receptor or family of receptors (such as the somatostatin family).

Affinity and potency: Where a range of affinities and potencies were reported, these are shown. Where peptides have affinities for more than one subtype within the family, all values are shown where available. For example, the relative importance of the affinities for the five different subtypes of somatostatin receptors in the therapeutic action is unclear and all values have been included. Data are derived from human receptors except where indicated from rat[†].

pK_i : negative logarithm to base 10 of the concentration of the competing ligand that would occupy 50% of receptors, determined in a competition binding assay.

pK_D : negative logarithm to base 10 of the equilibrium dissociation constant for ligand receptor interactions.

pIC_{50} : negative logarithm to base 10 of the concentration of competing agonist or antagonist that inhibits the binding of a radioligand by 50% in a competition binding assay.

pEC_{50} : the negative logarithm to base 10 of the molar concentration of an agonist that produces 50% of the maximal possible effect of that agonist.

Plasma half-life (min) and route indicates calculations based on intravenous administration. Clinical administration may also be via other routes such as intra-muscular or intra-nasal that may alter these values.

Volumes of distribution (L) have been recalculated where these were reported as litres/kg based on 70 kg body weight.

Synonyms are given for clinical names of the peptide based on the information in databases indicated.

Note 1. Human parathyroid hormone (1-84), manufactured as a recombinant form with the full 1-84 amino acids was approved for clinical use as Natpara, (ALX1-11, rhPTH1-84) but it is included as shorter sequences are also effective in activating target receptors. Teriparatide is a synthetic peptide comprising 1-34 of the N-terminal amino acids of human parathyroid hormone.

Supplementary Table 3 | **Modified peptides targeting Class A and B GPCRs that are approved for clinical use**

Family	Target Receptor	Ligand Mode of Action Approval Date	Clinical Indication	Affinity pK_i *pK_D **pIC_{50}	Potency pEC_{50}	Plasma Half-life (hr), iv *sc	Volume of Distribution (L) iv *sc	Plasma Binding (%)	Clearance (L/hr)	Route of Elimination	Synonyms
Class A											
Bradykinin	B_2	Icatibant Antagonist 2008	Hereditary Angioedema	10.2	8.0–9.4	1-2 *1.4	29	44	14.7±4.0	Proteolytic Enzymes	D-Arg-[Hyp^3,Thi^5,D-Tic^7,Oic^8]BK; HOE140;Firazyr
Cholecystokinin	CCK_2	Pentagastrin Agonist 1974	Diagnostic Aid	9.05	-	0.16 *<0.6	-	-	-	-	ICI-50123; AY-6608;Peptavlon
Gonadotrophin-Releasing Hormone	$GnRH_1$	Buserelin Agonist 1999	Endometriosis, Pituitary Desensitisation Prior to Ovulation Induction, Advanced Prostate Cancer	9.4-10.0 *9.5-10.4	10.5	0.08-1.3 *1.33	-	15	-	Proteolytic Enzymes	HOE 766; HOE 766A; ICI 123215 Suprefact; Receptal; Etilamide; Metrelef
		Cetrorelix Antagonist 1999	Controlled Ovarian Stimulation	9.3-10	8.7	*5-62.8	81	86	5.4	Renal	SB-075; Cetrotide
		Ganirelix Antagonist 2003	Controlled Ovarian Stimulation	-	-	14.5 *13-16	43.7	82	2.4	Renal, Biliary	Antagon; Orgalutran; Fyremadel; RS 26303
		Degarelix Depot Antagonist 2008	Advanced Prostate Cancer	8.8	-	996-1690 *696	40.9	90	-	Faecal (70-80%), Renal (20-30%)	FE200486; Firmagon
		Gonadorelin Agonist 1986	Amenorrhea, Hypogonadism.	-	-	0.16-0.67	-	-	-	Metabolism by Hydrolysis	Abbott 41070; AY-24031; Hoe-471; RU-19847
		Goserelin Agonist 1989	Breast Cancer, Prostate Cancer	8.8	-	4.9	44.1 *13.7	27	7.3±2.5	Renal, Biliary	Decapeptide I; ICI 118630; Zoladex
		Histrelin Agonist 2004	Advanced Prostate Cancer	8.7-9.7 *9.0-10.4	-	*4	58	30	10.4		Supprelin LA; Vantas; ORF 17070; RWJ 17070
		Leuprolide Agonist 1985	Advanced Prostate Cancer	8.5-9.1	-	3	27	43-49	8.3	Renal	Leuprorelin; Lupron; Viadu

											ABBOTT-43818; TAP-144; Eligard; Carcinil; Prostap Lutrate
		Nafarelin Agonist 2005		10	-	3	-	80	-		Synarel
		Triptorelin Agonist 1986	Prostate Cancer, Endometriosis, Precocious Puberty	8.5-8.8	-	3 phases 0.1, 0.75, 3	30-33	0	12.7	Renal, Biliary	Triptodur; Trelstar; Pamorelin; CL-118532; Decapeptyl; Diphereline; Gonapeptyl; Variopeptyl
		Abarelix Antagonist 2003 **Note 1**	Prostate cancer	9.1-9.5	-	317±77	-	96-99	-	-	PPI 149; R 3827; Plenaxis
Melanocortin	MC_1 MC_3 MC_4 MC_5	Afamelanotide Agonist 2014	Erythropoietic Protoporphyria	**10.0 8.9 8.5–8.8 **9.0	-	0.8-1.7	-	-	-	-	Scenesse
	MC_1 MC_3 MC_4 MC_5	Bremelanotide Agonist 2018	Sexual Arousal Disorder	- - **8.0 -	-	2	-	-	-	-	PT-141; Rekynda
Opioid	κ	Difelikefalin Agonist 2019	Post Abdominal Surgery Pain	-	9.8	2	-	-	-	Unchanged in Bile and Urine	CR-845
Relaxin	RXFP1	Serelaxin Agonist 2016	Heart failure	**10	9.2	8-9	0.3-1.0	-	0.12-0.14	Proteolytic Enzymes	Reasanz; RLX-030 Recombinant Human Relaxin 2
Somatostatin	SST_1 SST_2 SST_3 SST_5	Pasireotide Agonist 2012	Agromegaly, Cushing's Disease	**8.0 **9.0 **8.8 **9.8	-	12	>100.	88	-	Mainly Hepatic, Renal	SOM 230; Signifor
	SST_1 SST_2 SST_3 SST_5	Lanreotide (DEPOT) Agonist 1994	Agromegaly, Gastroentero-Pancreatic Tumours	**6.7 8.7-9.6 7.2-8.0 7.4-9.3	-	1.14 *528	16	-	23.7	Billiary, Renal (<5%)	DC 13-116; Somatuline; Ipstyl; BIM 23014; Lanreotide acetate

	SST_2 SST_3 SST_5	Octreotide Agonist 1987	Agromegaly, Gastroentero- Pancreatic Tumours	8.7-9.9 7.4-8.6 7.2-9.5	-	1.67 *4.2	13.6	65	7.6	Mainly Hepatic, Renal	DRG-0115; Longastatin; SMS 201 995; Sandostatin; Atrige; Sandostatin LAR, Lutathera **Note 2**
	SST_2 SST_3 SST_5	Vapreotide Agonist 2009	Oesophageal Variceal Bleeding	8.3-10.1 7.4-7.9 7.3-9.2	-	0.5	-	-	-	Mainly Hepatic, Renal	BMY 41606; CCRIS 6495; RC-160; Sanvar IR; Vapreotide acetate
Vasopressin and Oxytocin	OT	Atosiban Antagonist 2000	Delaying Imminent Pre-Term Birth	6.0-7.6	-	1.7	18 l	46-48	41.8	Proteolytic Enzymes	ORF22164; RWJ 22164 d[D-Tyr(Et)2, Thr^4,Orn^8] vasotocin d [D-Tyr(Et)^2 Thr^4]OVT; Tractocile; Antocin
	OT V_{1A} V_{1B} V_2	Desmopressin Agonist 1999	Vasopressin- Sensitive Cranial Diabetes Insipidus, Post Hypophysectomy Polyuria/Polydipsia.	6.7-7.6 7.0-7.7 7.7-8.2 7.2-8.6	-	0.9-2.6	33	17-50	-	Renal	1-deamino,D-AVP [deamino-Cys1,D-Arg^8]vasopressin dDAVP; Adiuretin; Concentraid; Minirin; Stimate; Noctiva
	V_{1A}	Felypressin Agonist 1969	Haemostatic Agent	-	-	-	-	-	-	-	PLV-2
	V_{1A} V_{1B} V_2	Terlipressin Agonist 2006	Hypotension, Bleeding Oesophageal Varices	-	-	0.4-1.1	35	30	37.8	-	Glypressin; Lucassin
	OT	Carbetocin Agonist 2016	Postpartum Haemorrhage	-	-	1.4-1.7	-	-	-	Partly Proteolytic Enzymes, Negilible Renal	Duratocin Pabal Lonacten; Depotocin; Comoton Decomoton
Class B											
Calcitonin	AMY_1	Calcitonin (Salmon) Agonist 1976	Paget's Disease	**8.7-9.7	10.0	*1-1.1	16	30-40	-	Renal	Fortical; Miacalcin
	CT	Elcatonin Agonist 1981	Pain Caused by Osteoporosis	-	-	-	-	-	-	-	

	AMY_1 AMY_2 AMY_3 CT	Pramlintide Agonist 2005	T1DM, T2DM	-	9.4 8.6-8.9 9.1-9.3 8.3	0.4-0.7 *0.8	56	60	60	Renal	AC-0137; AC-137; Symlin; Symlinpen
Glucagon	GHRH	Sermorelin Agonist 1990 **Note 3**	Dwarfism, HIV-Associated Weight Loss	8.2	-	0.17 *0.2	24-26	-	144-168	-	Sermorelin Acetate; Geref
		Tesamorelin Agonist 2010	HIV-Infected Patients with Lipodystrophy.	10.2	-	*0.43	*658	-	-	-	TH9507; (3E)-hex-3-enoylsomatoliberin; Egrifta
	GLP-1	Albiglutide Protein Fused Agonist 2014	HIV-Infected Patients with Lipodystrophy.	-	†7.7	*96-168	*11	-	0.07	Human Serum Albumin, Catabolized Primarily in Vascular Endothelium.	GSK-716155; Eperzan; Tanzeum
		Dulaglutide Agonist 2014 **Note 4**	T2DM	-	-	*120	*17-19	-	0.11	-	GLP-1Fc; LY2189265; Trulicity
		Exenatide Agonist 2005	T2DM	8.7-9.0 **9.2	-	*2.4	*28.3	-	9.1	Renal	Exendin-4, AC002993; AC 2993; AC2993A; Byetta; Bydureon;
		Liraglutide Agonist 2009	T2DM	8.3-10	10.2	*13	4.9 *11-17	>98	1.2	Proteolytic Enzymes	NN-2211; Victoza; Saxenda
		Lixisenatide Agonist 2013	T2DM	8.9	-	*3	*100	55	35	Proteolytic Enzymes	Adlyxin; AVE-0010; Lyxumia
		Semaglutide Spacer Agonist 2017	T2DM	-	11.2	*168	*9.4	99	0.04	Renal	NN-9535; Ozempic
	GLP-2	Teduglutide Agonist 2012	Short Bowel Syndrome	**†11.3	10	2.0	7.2 *26	-	8.6	Renal	ALX-0600; Gattex; Revestive; (Gly2)GLP-2;
Parathyroid Hormone	PTH1	Abaloparatide Agonist 2017	Post-Menopausal Osteoporosis	**9.7	10.1	*1.7	50	70 (in vitro)	-	Renal	BA058; Tymlos

Class C											
Calcium-Sensing	CaS	Etelcalcetide Agonist 2016	Secondary Hyper-Parathyroidism	-	4.6	84 *72-96	796	47	7.7	Renal	Velcalcetide KAI-4169 AMG-416 Parsabiv

Class, Target Receptor and Ligand. Compilation of the data used the same databases and methods as outline in Table 1. The table reflects the consensus that synthetic peptides act primarily on a single receptor or family of receptors (such as the somatostatin family). Cyclosporin reported to be an antagonist of formylpeptide FPR1 receptor has been omitted as it is reported to interact with multiple targets and is not selective for a particular target.

Clinical indication. These represent the main clinical uses in DrugBank[210], RxList[211], Electronic Medicines Compendium[213] and Clinical Trials.Gov[214].

Affinity and potency: Where a range of affinities and potencies were reported, these are shown. For peptides binding to somatostatin receptors, the relative importance of the affinities for the different subtypes in the therapeutic action is unclear and all values have been included. Data are derived from human receptors except where indicated (†) where values at the rat receptor are reported.

Plasma half-life (hr): time taken for the concentration of a drug in plasma to decline to half its original level.

Route: indicates calculations based on intravenous and sub-cutaneous administration. Clinical administration for a small number of peptides may also be via other routes such as intra-muscular or intra-nasal and can alter these values. For example, calcitonin (salmon) plasma half-lives are: intra-muscular, 0.96 hr, intra-nasal 0.3-38 hr.

Volumes of distribution (L): Where values were reported as L/kg these have been recalculated based on 70 kg body weight.

Plasma binding (%): The percentage of peptide bound to blood proteins including human serum albumin, lipoprotein, glycoprotein, and α, β, and γ globulins.

Clearance (L/hr): Where values were reported as L/hr/kg, these have been recalculated based on 70 kg body weight**.**

Route of Elimination: The main routes of metabolism and/or elimination are reported**.**

Synonyms are given for clinical names of the synthetic peptide based on the information in databases indicated.

NA: Not available

Note 1. Abarelix was discontinued in United States in 2003, owing to allergic reactions but clinical use has continued in Europe.

Note 2. Lutathera is a radiolabelled peptide that exploits radiation to kill tumours.

Note 3. Withdrawn in United States.

Note 4. Dulaglutide contains GLP-1(3- 37) with substitutions Ala8Gly, Gly22Glu, Arg36Gly, 16 amino acids linker sequence and 228 amino acid synthetic human Fc fragment (immunoglobulin G4). Two identical peptide chains form a dimer, linked by inter-monomer disulphide bonds between Cys55-55 and Cys58-58.